

Performance Analysis of Phase Estimation Algorithms for Interferometric Data

Dr. M. M. Mohamed Ismail¹, Dr. M. M. Mohamed Sathik²

¹Assistant Professor, Department of Computer Applications, The New College, Chennai

²Principal, Sadakathullah Appa College, Tirunelveli

Email address: mohammedismi@gmail.com

Abstract—Atmospheric turbulence strongly affects the performance of ground based telescope images. Shearing Interferometry based wavefront sensor is widely used for atmospheric turbulence correction in adaptive optics systems. In this paper, we simulated a noisy interferometric image based on polarized shearing interferometer which is affected by Kolmogorov turbulence. The phase extraction from noisy interferometric fringe pattern using different transform methods are described. The principles of Fourier transform (FT), windowed Fourier transform (WFT) and wavelet transform (WT) methods for phase extraction are discussed.

Keywords— Adaptive Optics, Shearing Interferometer, Fourier transform, windowed Fourier transform and wavelet transform.

I. INTRODUCTION

In Astronomical Instrumentation, the medium is the Earth's turbulent atmosphere, and the optical signal is the light emitted by the star or the body of interest. The atmospheric turbulence can be considered as a random process and can be estimated by means of variances and co-variances of local refractive index fluctuations [1]. Due to change in the refractive indices of the different layers, the planar wavefront, from the distant star, propagating through the turbulent atmosphere, gets distorted. So, both the amplitude and phase of the incoming beam fluctuate during its passage and changes with time. Thus, the random process of the atmospheric turbulence, affect the image forming capabilities of the telescope. The effects of turbulence on light that passes through the atmosphere are three types.

- It creates intensity fluctuations or scintillations which are observed as the twinkling of the stars.
- The position of the star wanders when the varying refractive index of the atmosphere alters the angle of arrival of the starlight.
- There is a spreading effect created by the higher order aberrations which causes stars to appear as small discs of light and not sharply defined point sources.

To resolve atmospheric turbulence for ground based telescope, Adaptive Optics (AO) technology was developed by astronomers [2,3]. It is a technique which measures the wavefront phase errors generated by the variations of the index of refraction in the atmosphere and corrects the resulting image in real time to achieve an angular resolution close to the diffraction limits of the telescope. The major components involved in a simple Adaptive Optics system are Wavefront Sensor which measures phase variations, Wavefront Correction device (Deformable Mirror), control algorithm and hardware which must be very fast to correct real-time variations.

A Wavefront Sensor is a device that helps in determining the shape of the incoming beam. Wavefront Corrector is a phase distortion compensation tool. The control algorithm takes the input from the Wavefront Sensor and translates the

information into command values that can be addressed to the Wavefront Corrector. Various Wavefront Sensing techniques have been developed for use in a variety of applications ranging from measuring the wavefront aberrations of human eyes [4] to Adaptive Optics in astronomy [5]. The most commonly used Wavefront Sensors are the Shack-Hartmann (SH) [6, 7], Curvature sensing [8], Lateral Shearing Interferometry (LSI) [9, 10 and 11], Phase Retrieval methods [12] and Pyramid Wavefront Sensor [13]. It is important to understand the Polarization Shearing Interferometer (PSI) theoretically to sense the wavefront errors. For this purpose, a simulation of wavefront has been generated and incorporated the wavefront errors caused due to atmospheric turbulence.

II. SIMULATION OF NOISY INTERFEROMETRIC FRINGE PATTERN

Based on equation given 2.1 and which is explained at [14] an interferometric image was simulated as shown in figure 1.

$$W(x, y) = A(x^2 + y^2)^2 + By(x^2 + y^2) + C(x^2 + 3y^2) + D(x^2 + y^2) + Ey + Fx \quad (2.1)$$

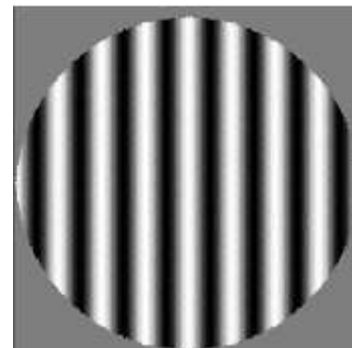


Fig. 1. Typical Polarization Shearing Interferogram

Gaussian noise is evenly distributed over the signal. This means that each pixel in the noisy image is the sum of the true pixel value and a random Gaussian distributed noise value. As the name indicates, this type of noise has a Gaussian

distribution, which has a bell-shaped probability distribution function given by,

$$\frac{1}{\sigma\sqrt{2\pi}} \exp\left(-\frac{(x-\mu)^2}{2\sigma^2}\right) \quad (2.2)$$

where x represents the gray level, μ is the mean or average of the function and σ is the standard deviation of the noise. Varying sigma for the Gaussian noise in the interferogram the distorted image has been produced. The Figure 2 shows the noisy interference fringe pattern with varying Gaussian Noise Level of 0.1, and 2, for respective a, b.

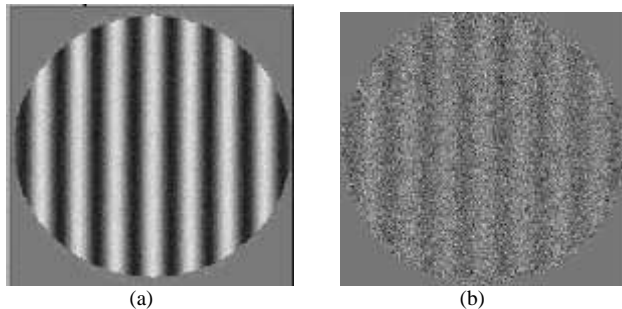


Fig. 2. Noisy Interferogram with Gaussian Noise Level of 0.1(a) and 2(b).

2.1 Kolmogorov Model of Atmospheric Turbulence

The most widely accepted theory of turbulence flow, due to consistent agreement with observation, was first put forward by Andrei Kolmogorov [15]. It assumes that energy injected into turbulent medium on large spatial scales (outer scale, L_0) and forms eddies. These large eddies cascade the energy into small scale eddies until it become small enough (small scale, l_0) that the energy is dissipated by the viscous properties of the medium. The inertial range between inner and outer scales Kolmogorov predicted a power law distribution of the turbulent power with spatial frequency, κ ($\sim 11/3$). In order to accommodate the finite inner and outer scales, the Kolmogorov power spectrum was modified by Von Karman power spectrum [16] which is given by.

$$\phi_N(\kappa) = 0.033C_N^2 (\kappa^2 + \kappa_0^2)^{-11/6} \exp(-\kappa^2 / \kappa_i^2) \quad (2.3)$$

Where $\kappa_0 = 2\pi / L_0$, $\kappa_i = 5.92 / l_0$ and $\kappa = 2\pi / L$. It can be expressed in another form with Fried parameter r_0 ,

$$\phi_N(\kappa) = 0.023(D / r_0)^{5/3} \frac{\exp(-\kappa^2 / \kappa_i^2)}{(\kappa^2 + \kappa_0^2)^{11/6}} \quad (2.4)$$

For infinite outer scale ($\kappa_0 = 0$) and zero inner scale ($\kappa_i = \infty$) above equation reduces to,

$$\phi_N(\kappa) = 0.023(D / r_0)^{5/3} \kappa^{-11/3} \quad (2.5)$$

Where D is Telescope Diameter and r_0 is fried parameter and the Power Spectral density (PSD) and phase screen $f(r)$ are related as,

$$\phi_N(\kappa) = \left| \int_{-\infty}^{\infty} f(r) e^{-i\kappa r} dr \right|^2 \quad (2.6)$$

From the above equation phase screen is derived by:

$$f(r) = \int_{-\infty}^{\infty} \sqrt{\phi_N(\kappa)} e^{i\kappa r} d\kappa \quad (2.7)$$

Where $f(r)$, is the two dimensional Kolmogorov phase screen, which can be obtained from inverse Fourier Transform of the square root of Von Karman power spectrum of turbulent atmosphere.

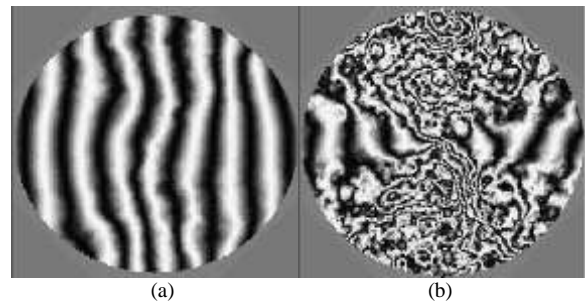


Fig. 3. Interferogram with Kolmogorov turbulence affected with $D/r_0 = 0.1$ (a) and $D/r_0 = 2$ (b)

III. PHASE EXTRACTION

In real-time the interferogram is affected due to atmospheric turbulence. We simulated an interferometric image and it is affected by Kolmogorov turbulence including Gaussian noise which we described in the previous section. Due to inclusion of the turbulent phase in the interferogram, the image disturbed and it is important to retrieve phase information from fringes and data reduction for further process of wavefront error estimation and correction.

The phase is the required information from the distorted wavefront. While extracting the phase unwanted information (noise) was removed. By removing noise, the phase was retrieved and wavefront error map was generated. This section gives details of algorithm which we developed for phase estimation of an interferogram image by Fourier Transform approach, wavelet based approach and windowed Fourier Transform Method using LabVIEW. This paper compares these techniques in terms of their noise performance, reliability and the required time to execute using computers. A comparative study of the three proposed algorithms based on their denoising performance, accuracy, reliability and the computation time for phase retrieval using LabVIEW has been done.

IV. PHASE EXTRACTION THROUGH FOURIER TRANSFORM

There are various methods to estimate the phase from the distorted or noisy fringe pattern. One way to quickly filter a dataset without much effort is to use a Fast Fourier Transform (FFT). A FFT is a way to decompose a signal into a sum of sine waves. The amplitude and phase associated with each sine wave is known as the spectrum of a signal. If the spectrum of the noise is away from the spectrum of the original signal, then original signal can be filtered by taking a FFT. Then Inverse Fast Fourier Transform (IFFT) was used to reconstruct the signal. Fourier analysis approach has been adopted for the determination of local phase of the proposed PSI interferogram [17, 18]. The FFT method is resistant to noise and is highly efficient and very simple to apply [19].

The one-dimensional plot of the distorted fringe pattern was considered. The FFT Technique was applied to the one-dimensional plot to find out the original signal after removing the entire unwanted signal. To remove all the higher frequencies and unwanted signals, the power spectrum of the FFT plot was calculated. The frequency that contains the maximum information was only considered and all the other frequencies were neglected. Then the IFFT of the above signal that contained the maximum information was found out to get back the signal in terms of the spatial co-ordinates and the image was filtered. In frequency domain the data was fitted into the band pass filter which removed both high and low frequency.

4.1 Algorithm Implementation using Fourier Transform

```

Begin
Step - 1
    Generate a noiseless interference fringe pattern
Step - 2
    Fourier Transform-based Phase Screen
Step - 3
    Convolve step 1 and step 2
    Generate a noisy interference fringe pattern
Step - 4
    Phase Extraction using Fourier Transform
    For i = 1 to 256
    {
        Take 1D data
        Fit into Fast Fourier Transform
        Remove both low and high frequency
        Allow only the information and neglect
        the remaining
        Take IFFT of that maximum information
    }
Step - 5
    Store the 1D data into 2D data
    Plot the 2D Data
End
    
```

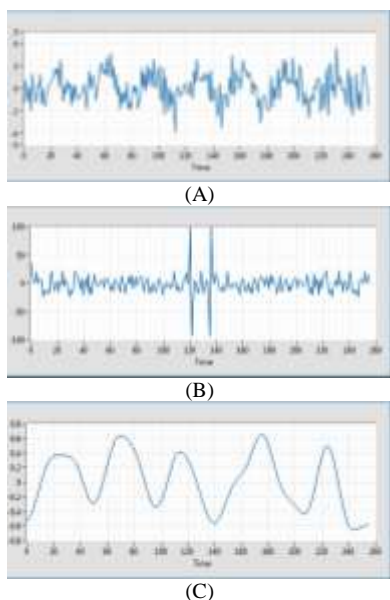


Fig. 4. One Dimensional Plot for (A) Noisy data and (B) its Fourier Transform, (C) Inverse Fourier Transform

The Figure 5.A shows the noisy interferogram with Gaussian noise of 0.5 and its filtered image is shown in Figure 5.B using Fourier Transform. The Figure 5.C shows the noisy interferogram affected by turbulent phase screen of $D/r_0 = 1$ with Gaussian noise of 0.5 and its filtered image is shown in Figure 5.D using Fourier Transform developed by the above algorithm.

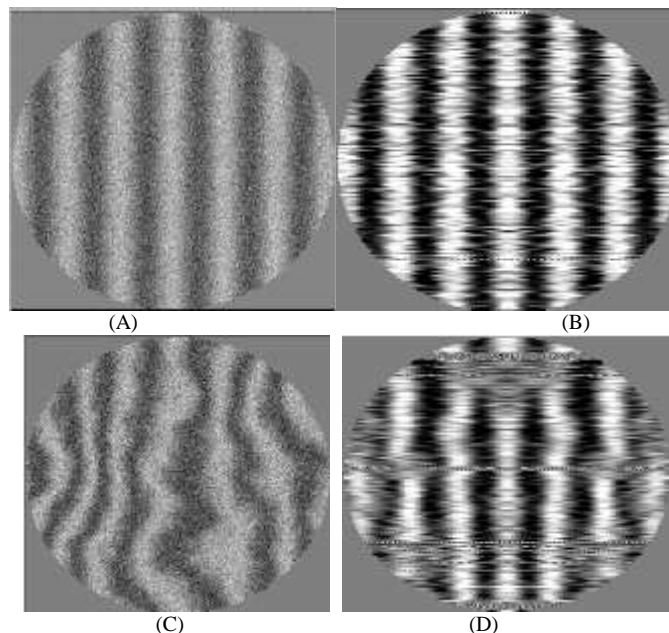


Fig. 5. The Noisy Image and Filtered Image using Fourier Transform with Band Pass Filter

V. PHASE EXTRACTION THROUGH WAVELET TRANSFORM

Wavelet Transform (WT) is one of the most important and powerful tools of signal representation. It has been used in image processing, data compression, and signal processing. The Wavelet based approach finds applications in denoising images corrupted with Gaussian noise. The methods of Wavelet analysis are studied in order to reduce unwanted noise signal from digital signals. The Wavelet Transform decomposes signals over dilated and translated functions called Wavelets, which transform a continuous function into a highly redundant function.

The Wavelet Transformation is representation of images in two dependant domains, by which a localization of the Wavelet basis functions in both time and frequency domain leads to multi resolution analysis and filter designs of specific application [20]. Most of the properties of the Wavelet Transformation make it very effective for denoising. The decomposition of a data or an image into some Wavelet coefficients is called Wavelet thresholding. The detailed coefficients are compared with a given threshold value and then these coefficients are shrink close to zero for denoising the image. During the thresholding process, a Wavelet coefficient is compared with a given value and is set to zero if its value is less than threshold. There are two general categories of thresholding namely hard-thresholding and soft-thresholding [21].

5.1 Algorithm Implementation using Wavelet Transform

```

Begin
Step - 1
    Generate a noiseless interference fringe pattern
Step - 2
    Fourier Transform-based Phase Screen
Step - 3
    Convolve step 1 and step 2
    Generate a noisy interference fringe pattern
Step - 4
    Phase Extraction using Wavelet Transform
    For i = 1 to 256
    {
    Take 1D data and Fit into Morlet Transform
    Find ridge from the modulus array
    Find maximum value of each column in the modulus
    array
    Phase is chosen from the corresponding phase array
    }
Step - 5
    Store the 1D data into 2D data
    Plot the 2D Data
End
    
```

The Figure 6.A shows the noisy interferogram with Gaussian noise of 0.5 and its filtered image is shown in Figure 6.B using Wavelet Transform. The Figure 6.C shows the noisy interferogram affected by turbulent phase screen of $D/r_0 = 1$ with Gaussian noise of 0.5 and its filtered image is shown in Figure 6.D using Wavelet Transform developed by the above algorithm.

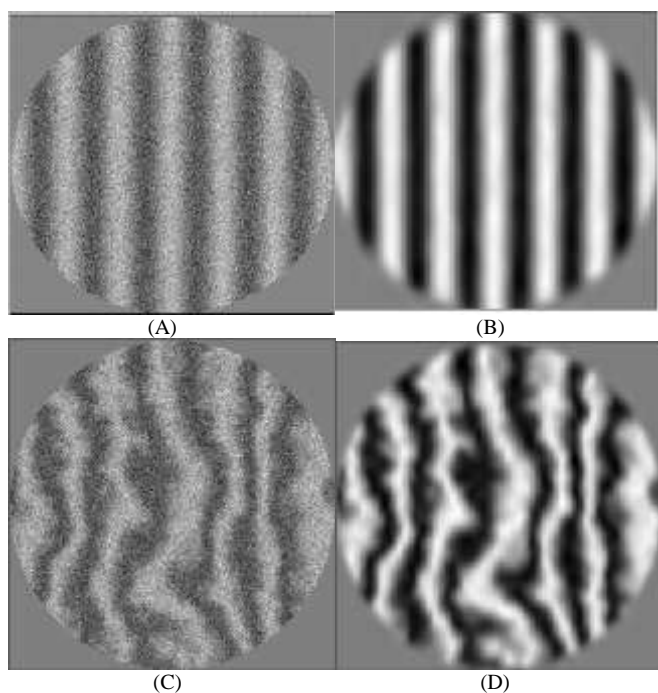


Fig. 6. The Noisy Image and Filtered Image using Morlet Wavelet Transform

VI. PHASE EXTRACTION THROUGH WINDOWED FOURIER TRANSFORM

The procedure for computing Windowed Fourier Transform (WFT) is to divide a longer time signal into shorter segments of equal length and then compute the Fourier Transform separately on each shorter segment. This reveals the Fourier spectrum on each shorter segment. The Windowed Fourier Transform is also called the Short Time Fourier Transform (STFT), or the Sliding Fourier Transform which partitions the time-domain input signal into several disjointed or overlapped blocks by multiplying the signal with a window function and then applies the discrete Fourier Transform to each block. The WFT is computationally efficient because it uses the Fast Fourier Transform (FFT) [22, 23 and 24].

For phase estimation, a one dimensional noisy fringe pattern was fitted to the Windowed Fourier Transform which was transformed into spectrum. The noise permeated the whole spectrum domain with very small coefficients due to its randomness and incoherence with the WFT basis. This was suppressed by discarding the spectrum coefficients if their amplitudes were smaller than a preset threshold. A smooth image was produced after an Inverse Windowed Fourier Transform (IWFT). The WFT and IWFT can be written as [25]

$$Sf(u, \xi) = \int_{-\infty}^{\infty} f(x) g(x-u) \exp(-j\xi x) dx, \quad (4.10)$$

$$f(x) = \frac{1}{2\pi} \int_{-\infty}^{\infty} \int_{-\infty}^{\infty} Sf(u, \xi) g(x-u) \exp(j\xi x) d\xi du \quad (4.11)$$

Where $Sf(u, \xi)$ denotes the WFT spectrum; $g(x)$ is a window, which can be chosen as a Gaussian function,

$$g(x) = \exp(-x^2 / 2\sigma^2) \quad (4.12)$$

In a Fourier Transform, when $f(x)$ was transformed to $Ff(\xi)$, the frequency information was maintained but time information was lost and can hardly be recognized (i.e) $Ff(\xi)$ was possible to find frequencies that appear from the spectrum, but not where they occur in the signal. But using WFT, $Sf(u, \xi)$ was possible to know not only the spectrum components but also where a component appeared in the time domain. The WFT has advantages over Fourier Transform as it is performed over a local area. It was determined by the extension of $g(x)$, where a signal in one position will not affect the signal in another position. In spectral analysis, the spectrum of the signal in a local area was simpler than the spectrum of the whole field signal hence more effective operation of the spectrum was possible.

6.1 Algorithm Implementation using WFT

```

Begin
Step - 1
    Generate a noiseless interference fringe pattern
Step - 2
    Fourier Transform-based Phase Screen
Step - 3
    Convolve step 1 and step 2
    Generate a noisy interference fringe pattern
    
```

```

Step - 4
Phase Extraction using Wavelet Transform
For i = 1 to 256
{
Take 1D data and Fit into WFT
Transfer data into spectrum
Eliminate noise by thresholding
Take Inverse WFT
}
Step - 5
Store the 1D data into 2D data
Plot the 2D Data
End

```

The Figure 7.A shows the noisy interferogram with Gaussian noise of 0.5 and its filtered image is shown in Figure 7.B using Windows Fourier Transform. The Figure 7.C shows the noisy interferogram affected by turbulent phase screen of $D/r_0 = 1$ with Gaussian noise of 0.5 and its filtered image is shown in Figure 7.D using Windows Fourier Transform developed by the above algorithm.

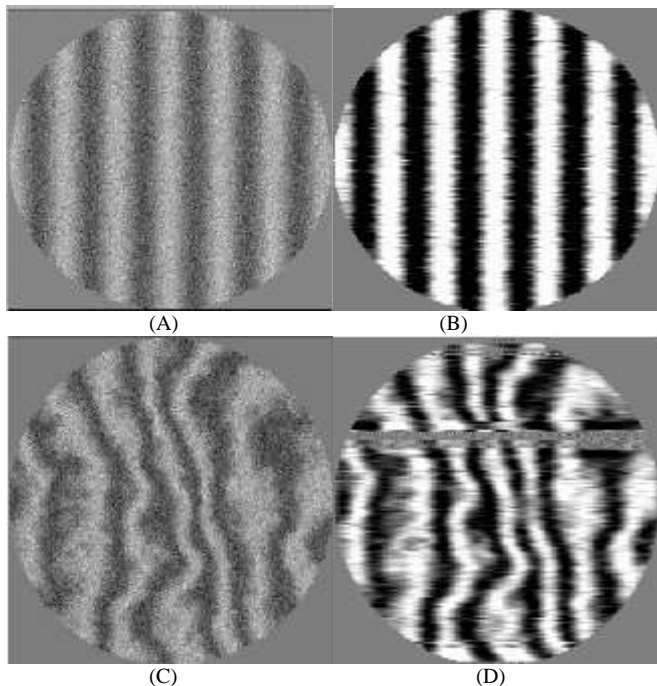


Fig. 7. The Noisy Image and Filtered Image using WFT

VII. CONCLUSION

This paper has presented a complete simulation of interferometric image based on shearing interferometer and noisy interferometric. It also described about the phase estimation using fourier transform, wavelet transform and windows fourier transform. The SNR calculated after the noise was filtered using Fourier Transform algorithm was 2.3 db. The noise was not completely reduced and it is slightly better than existing algorithms. The SNR calculated for the filtered image using 1D Morlet Wavelet Transform was 2.9 db. From the Figure 5 one can see that 1D Morlet Wavelet Transform performs better in straight fringe condition and it is not performed well with the curved fringes which are affected by

Kolmogorov turbulence. The SNR calculated after filtering the image using WFT algorithm was 3.4 db. The noise was drastically reduced compared to other algorithms.

All the algorithms were programmed in the LabVIEW platform and executed on Intel i3 Core computer with a 3.60 GHz clock speed and 4 GB -RAM. All the coding have been written by using data parallelism and parallel processing through pipelining for optimizing the computation speed. By using pipelining in LabVIEW programming, it is worth underlining that an additional gain of a factor 4 to 5 in the computation time is achieved. The improved algorithm is much faster than the existing one with reduced computation time.

REFERENCE

- [1] J. W. Hardy, Adaptive Optics for Astronomical Telescopes, 1998.
- [2] H. W. Babcock, "The possibility of compensating astronomical seeing. Public of the Astron.," *Soc. Pac.*, vol. 65, pp. 229-236, 1953.
- [3] J. W. Hardy, "Adaptive optics: A new technology for the control of light," *Proc. IEEE*, vol. 66, issue 6, pp. 651-697, 1978.
- [4] M. Lombardo and G. Lombardo, "New methods and techniques for sensing the wave aberrations of human eyes," *Clinical and Experimental Optometry*, vol. 92, issue 3, pp. 176-186, 2009.
- [5] F. Roddier, Adaptive Optics in astronomy, Cambridge university press, Cambridge, United Kingdom, 1999.
- [6] B. C. Platt and R. V. Shack, "History and principles of Shack-Hartmann wavefront sensing," *Journal of Refractive Surgery*, vol. 17, S573-S577, 2001.
- [7] R. V. Shack and B. C. Platt, "Production and use of a lenticular Hartmann screen," *J. Opt. Soc. Am.*, vol. 61, pp. 656-660, 1971.
- [8] E. Roddier, "Curvature sensing and compensation: A new concept in adaptive optics," *Appl. Opt.*, vol. 27, pp. 1223-1225, 1988.
- [9] J. W. Hardy and A. J. MacGovern., "Shearing interferometry: A flexible technique for wavefront measurement," *Proc. SPIE 0816, Interferometric Metrology*, pp. 180-195, 1987.
- [10] J. E. Greivenkamp, and J. H. Bruning, "Phase shifting interferometers," in Optical Shop Testing, Ed., Malacara, D., Wiley Series, pp. 501-598, 1992.
- [11] E. Atad, J. W. Harris, C. M. Humphries, and V. C. Salter, "Lateral Shearing interferometry: Evaluation and control of the performance of astronomical telescopes" *SPIE 1236, Advanced Technology Optical Telescopes IV*, Lawrence D. Barr, Editors, 1990.
- [12] R. A. Gonsalves, "Phase retrieval and diversity in adaptive optics," *Opt. Eng.*, vol. 21, pp. 829-832, 1982.
- [13] R. Ragazzoni, and J. Farinato, "Phase retrieval and diversity in adaptive optics," *Opt. Eng.*, vol. 350, L23-L26, 1999.
- [14] M. Mohamed Ismail and M. Mohamed Sathik, "Imaging through Kolmogorov model of atmospheric turbulence for shearing interferometer wavefront sensor," *International Research Journal of Engineering and Technology (IRJET)*, vol. 2, issue 8, pp. 1217-1225, 2015,
- [15] A. N. Kolmogorov, "The local structure of turbulence in incompressible viscous fluid for very large Reynolds numbers (translation)," *Proceedings of the Royal Society of London A*, vol. 434, issue 1890, pp. 9-13, 1991.
- [16] C. Rao, W. Jiang, and N. Ling. "Spatial and temporal characterization of phase fluctuations in non-kolmogorov atmospheric turbulence," *Journal of Modern Optics*, vol. 47, issue 6, pp. 1111-1126, 2000.
- [17] M. Takeda, H. Ina, and S. Kobayashi, "Fourier Transform method of fringe-pattern analysis for computer based tomography and interferometry," *J. Opt. Soc. Am.*, vol. 72, issue 1, pp. 156-160, 1982.
- [18] C. Roddier and F. Roddier, "Interferogram analysis using Fourier transform techniques," *Appl. Opt.*, vol. 26, issue 9, pp. 1668-1673, 1987.
- [19] D. J. Bone, H. A. Bachor, and R. J. Sandeman, "Fringe pattern analysis using a 2-D fourier transform," *Appl. Opt.*, vol. 25, issue 10, pp. 1653-1660, 1986.
- [20] S. G. Chang, B. Yu, and M. Vetterli, "Adaptive wavelet thresholding for image denoising and compression," *IEEE Trans. Image Processing*, vol. 9, issue 9, pp. 1532-1546, 2000.

- [21] D. F. Guo, W. H. Zhu, Z. Gao, and J. Q. Zhang, "A study of wavelet thresholding denoising," *5th International Conference on Signal Processing Proceedings, WCCICSP*, pp. 329-332, 2000.
- [22] Q. Kema, "Windowed Fourier transform for fringe pattern analysis," *Applied Optics*, vol. 43, issue 13, pp. 2695-2702, 2004.
- [23] Q. Kema, H. Wang, and W. Gao, "Windowed Fourier transform for fringe pattern analysis: Theoretical analyses," *Applied Optics*, vol. 47, issue 29, pp. 5408-5419 2008.
- [24] K. Qian, S. H. Soon, and A. Asundi, "A simple phase unwrapping approach based on filtering by windowed Fourier transform," *Optics and Laser Technology*, vol. 37, issue 6, pp. 458-462, 2005.
- [25] K. Krochenig, *Foundations of Time-Frequency Analysis* Birkha user, Boston, 2001.